Int J Adv Manuf Technol (2016) 83:1395–1407
DOI 10.1007/s00170-015-7669-y

ORIGINAL ARTICLE

Analysis of forces and temperatures in friction spot stir welding of thermoplastic polymers

A. Paoletti[1] · **F. Lambiase**[1] · **A. Di Ilio**[1]

Received: 10 June 2015 / Accepted: 3 August 2015 / Published online: 14 August 2015

Abstract The present investigation analyses the force and torque developing during friction stir spot welding (FSSW) of thermoplastic sheets varying the main process parameters. In addition, measurements of the tool temperature and those of the material close to the welding region were carried out to better understand the variation of the forces during FSSW and quality of the joints. Experimental tests involving an instrumented drilling machine were performed on polycarbonate sheets. The study involved the variation of dwell time, tool plunge rate and rotational speed. Mechanical characterization and dimensional analysis of the joints were performed in order to assess the influence of the process parameters on the joint quality under considered processing conditions. According to the achieved results, using low values of the plunging speed has beneficial effects on both the process (reduction in the force and torque) and the mechanical behaviour of the joints. Increasing the tool rotational speed results in reduced processing forces and higher material mixing and temperature. The dwell time has a negligible effect on developing forces while it highly influences the material temperature, dimension of the welded region and consequently the mechanical behaviour of the joint.

Keywords Friction stir welding · Joining · Polymers · Thermoplastics · Polycarbonate · Forces · Temperature · Thin sheets · Plunge

✉ A. Paoletti
francesco.lambiase@univaq.it

[1] Department of Industrial and Information Engineering and Economics, University of L'Aquila, Monteluco di Roio 67040, Italy

1 Introduction

Thermoplastic materials are employed as structural components for replacing metals in a wide range of industrial fields including building, automotive and aerospace owing to a number of advantages including reduced cost of manufacturing, weight saving, flexibility and high thermal insulation. Besides the design flexibility, complex components usually involve many subparts being joined together. To this end, welding processes are generally employed; however, in order to overcome the principal limitations of such processes either improving the joint quality or reducing the processing time, new joining techniques are being developed to produce metal-polymer joints and polymer-polymer joints such as clinching [1, 2], self-pierce riveting [3], laser welding [4], friction press joining [5], friction riveting [6] and friction lap welding [7]. To ensure the mechanical performances of the assembled parts, the choice of the joining process is a key issue. Besides these processes, semisolid joining processes such as friction stir welding (FSW) and friction spot stir welding (FSSW) are achieving growing interest since they produce joints with high mechanical performances (the strength of the stirred zone is close to that of the base materials), a reduced heat-affected zone and reduced temperature (as compared to that of material fusion). In addition, the simplicity of the required machines, low energy consumption, no cover gas or external heating sources requirement have contributed to the diffusion of these processes and have pushed the researches to discover new fields of application. The difference between FSW and FSSW concerns the absence of the transverse speed; therefore, FSSW produces spot joints rather than continuous welds. In FSSW, frictional heat is generated by the interaction of the tool pin with the material that becomes pasty and extrudes vertically. The tool shoulder then exerts an upsetting action on the stirred material to form the weld nut. Since their initial employment

for joining materials being difficult to weld such as aluminium alloys, FSW and FSSW have been employed not only for a wider range of metals including titanium, magnesium, copper and even high-strength steels but also for different materials such as thermoplastics and composites. In addition, being semisolid, FSW and FSSW processes are less sensitive to either physical or chemical compatibility of the materials to join; thus, they are suitable for joining even dissimilar materials.

Since the initial development of such processes and employment for joining metals, a large number of studies have been presented on FSW and FSSW and their modelling [8–11] other than process parameters. Tool plunge rate during FSSW was investigated in [12]. Papahn et al. [13] investigated the effect of underwater FSW on translational force, temperature and mechanical behaviour of the welds. Rumulu et al. [14] analysed the influence of shoulder diameter and plunge depth on the formability of the sheet. Nevertheless, FSW and FSSW of thermoplastics involve different thermo-mechanical conditions from those developing in metal joining, owing to different rheological behaviour of such material [15]. Mostafapour and Azarsa [16] performed an experimental investigation on heat-assisted FSW of high-density polyethylene (HDPE) and found that the joints showed an ultimate tensile strength of 95 % of base material. Friction stir processing can be also employed for composite fabrication as reported in [17].

Olivera et al. [18] performed a preliminary study on the feasibility of friction spot welding in poly(methyl methacrylate) (PMMA). According to the achieved results, friction spot welds were characterized by higher shear strength with respect to those performed by means of microwave, thermal bonding and ultrasonic welding. Bilici et al. [19] investigated the influence of tool rotation speed, tool plunge depth and dwell time while joining of HDPE and determined the optimal combination of welding parameters. Bilici and Yükler [20] studied the effect of tool shape and found that a tapered cylindrical pin ensures better joint quality of the weld and yielded the highest weld strength over the analysed tool shapes. Memduh [21] investigated the effect of tool rotational speed, tool plunge rate, tool plunge depth, dwell time and waiting time on mechanical strength of FSSW joined made on polypropylene sheets. The research showed that the mechanical strength of FSSW joints was influenced by all the process parameters except the tool plunge rate. Hoseinlaghab et al. [22] studied the influence of the tool geometry on the creep behaviours of friction stir welded polyethylene plates and found that reducing the tilt angle improved the creep resistance of the welds. Pirizadeh et al. [23] developed a new tool involving two shoulders. The authors observed that the employment of such a tool allowed to eliminate root defect and back slit of the welded acrylonitrile butadiene styrene (ABS) parts. Panneerselvam and Lenin [24] studied the effect of a threaded pin profile while joining of Nylon 6 plates. Mendes et al. [25, 26] studied the morphology and strength of ABS welds performed by robotic FSW. Lambiase et al. [27] used artificial neural networks to determine optimal processing conditions of polycarbonate sheets using FSSW. Since the pioneer studies of FSSW of thermoplastics, a number of studies have been carried out on the feasibility of FSSW for joining dissimilar materials. Junior et al. [28] demonstrated the potential of friction spot welding for thermoplastic nanocomposite sheets by performing an experimental investigation on poly(methyl methacrylate) and poly(methyl methacrylate)-SiO2 nanocomposite. The authors also used friction spot joining to weld PMMA with PMMA/silica and PMMA/silica-g-PMMA nanocomposites functionalized via ATRP [29]. Goushegir et al. [30] analysed the mechanical strength and microstructure of friction spot joints of aluminium AA2024/carbon-fibre-reinforced poly(phenylenesulfide). Dashatan et al. [31] demonstrated the feasibility of hybrid joints made of PMMA to ABS thermoplastics using FSSW. The results indicated that the mechanical strength of welds was highly influenced by tool rotational speed, dwell time and tool plunge rate, the latter being the most effective parameter. In literature, there are no studies about the effects of the processing conditions on forces during friction spot stir welding of thermoplastic polymers except that of Bilici and Yükler [20]. However, the authors only analysed the influence of the tool geometry on the plunging force. Assessing the influence of the process parameters on developing forces and temperatures would be important for the determination of the machine requirements (motors, frame stiffness), especially for portable joining machines; however, any investigation has been yet carried out for friction stir welding of polymer materials. The knowledge of temperature arising during the process could allow improving the mechanical behaviour of the joints either reducing the overall process time. The adoption of an intelligent-instrumented machine could allow the selection of proper processing conditions, e.g. consolidation time and waiting time automatically in order to achieve a given mechanical strength of the joint within the minimum processing time.

The present study is aimed at analysing the influence of the main FSSW process parameters on the developing forces (plunging force and torque), tool and weld temperature other than the mechanical behaviour and geometry of the joints. Polycarbonate (PC) was used owing to its wide application as well as high mechanical strength and toughness. To this end, an instrumented drilling machine was employed to measure the forces developing during the joining operations. In addition, temperature measurements on the tool and the material near the welding area were performed. The study involved the variation of the dwell time, tool plunge rate and rotational speed. The variation of the characteristic regions of the welds (e.g. keyhole dimension, welded region and thermal affected zone) as a function of process parameters was also analysed.

2 Materials and methods

2.1 Experimental set-up

FSSW was performed to produce butt joints on polycarbonate specimens (100×20×3 mm). Polycarbonate is an amorphous thermoplastic polymer having high tensile strength and toughness. According to mechanical characterization performed in a previous work [1], the adopted sheets were characterized by a tensile strength of 60 MPa and an elongation at break of 110 %. The sheets were welded using an instrumented servo-drilling press shown in Fig. 1. The plunge motion is produced by means of a DC motor, while the tool rotational motion is produced by means of an asynchronous motor driven by an inverter. Plunge force *Fz* and torque *Mz* were measured by means of a two-component piezo-electric cell. The temperature of the tool and that of the material close to the welding region were measured to investigate the influence of the processing parameters on the developing temperatures. Particularly, the tool temperature was measured at 13 mm from the tool tip, as depicted in Fig. 1e by means of a pyrometer type 1060-2 connected to Thermophil INFRA type 4472 thermometer. The sheet temperature was measured by means of a K-type thermocouple (having a response time of 0.5 s). The thermocouple was placed between a wooden support and the lower surface of the bottom sheet in correspondence to the welding region, as depicted in Fig. 1e. Force and temperature signals were filtered by using a low-pass filter and were acquired by adopting a sample rate of 75 Hz.

A flat-end tool tip made of a low-carbon steel AISI 1010 was utilized in all the experimental tests. The tool had a shoulder with diameter of 11 mm, a pin with diameter of 5 mm and a pin length of 4.3 mm as depicted in Fig. 1d. FSSW can be ideally subdivided in four phases: preheating, plunging, consolidation and waiting prior to the tool retraction. The main FSSW phases are schematized in Fig. 2. The tool rotates at a prescribed speed (n) and is forced against the upper sheet to pre-heat the material for a set pre-heating time T_P with an interference depth of 0.1 mm. After the pre-heating time, the tool is forced against the underlying material at a constant plunging rate v_f and is stopped as the tool stroke reaches 4.9 mm. Then, the tool rotation proceeds to further time interval and stir the material within the welding region. This phase (consolidation) lasts for a prescribed time (T_D). Finally, the tool rotation terminates to cool down the pasty material.

According to the results achieved in previous works [32, 31], the mechanical strength of friction spot stir joints on polycarbonate sheets is mainly affected by the tool plunge rate, the tool rotation speed and the dwell time. On the other hand, the waiting time showed a threshold value above which the material was torn out from the joint since it was still pasty while higher values of waiting time had negligible influence on the joint strength. Similarly, the pre-heating time had negligible influence on the joint strength stem from the low thermal conductivity of the polymeric material. Thus, experimental tests were performed by varying the tool plunge rate, rotation speed and dwell time, one factor at a time over four levels and holding constant the other factors at an intermediate level. The investigated welding parameters and ranges are summarized in Table 1.

3 Results and discussion

3.1 Analysis of forces and temperature trends

Figure 3 depicts the variation of the acquired signals, i.e. plunging force (*Fz*) torque (*Mz*), temperature of the material,

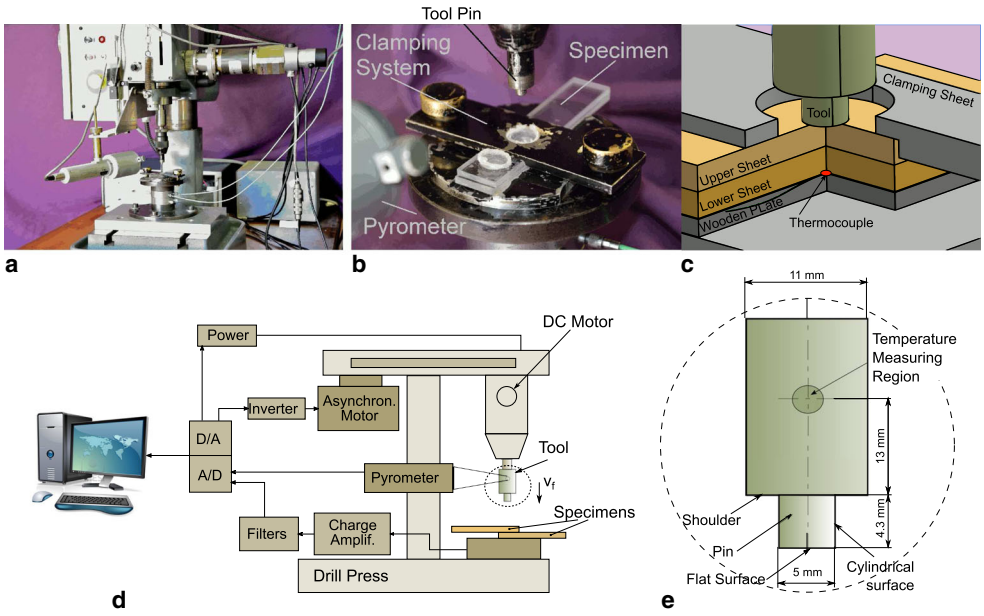

Fig. 1 **a** Picture of the experimental equipment, **b** layout of clamping system, **c** specimen setup, **d** schematic representation of instrumented servo-drilling press and **e** geometry of the tool tip used in the experiments

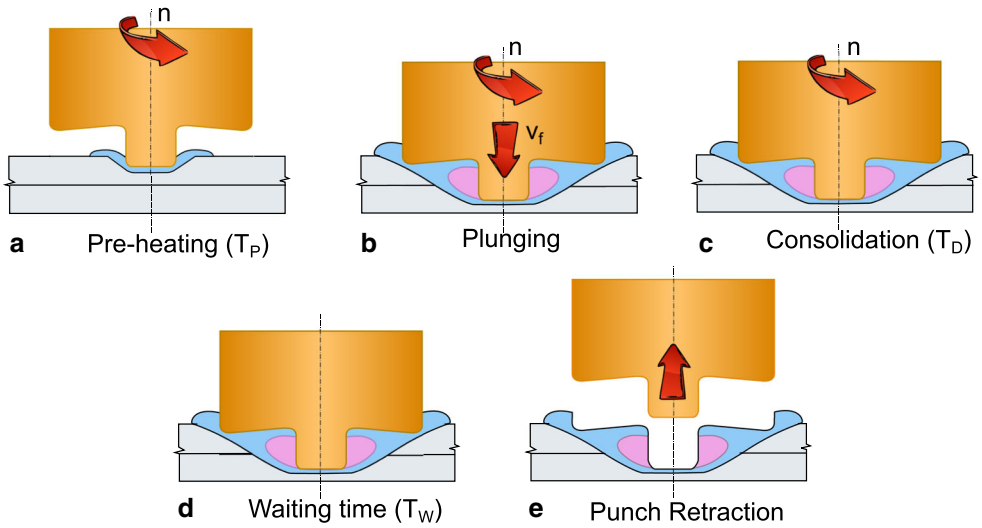

Fig. 2 Typical phases of friction stir spot welding process: pre-heating, joining, consolidation and tool retraction

measured at the bottom surface of the lower sheet (TM) and the temperature of the tool (TT).

At the beginning of the process (pre-heating and plunging phases), the temperature measured by the thermocouple remains unchanged, due to the long distance of the heated surface (in contact with the tool-tip extremity) from the measurement position and to the low thermal conductivity of polycarbonate. As the tool tip enters in contact with the bottom sheet (at the end of the plunging phase), the temperature measured begins to rise since the lower distance between the heated region and the thermocouple position. As the plunging motion stops (beginning of the consolidation phase), the tool rotation proceeds and the temperature further increases since the punch continues to rotate, producing further frictional heat. When the punch rotation stops (beginning of the waiting time), the temperature of the material near the welding region drops down and the pasty material begins to become harder. The selection of proper waiting time should ensure the correct solidification of stirred material in order to avoid the damage of the welding region and the material being torn out from the joining area, as shown in Fig. 4.

A different trend is shown by the temperature measured on the tool (Fig. 3). Indeed, during the plunging phase, the tool temperature rises gently since the thermal inertia of the tool material and the distance between the tool tip and the temperature measuring region. The tool temperature grows up owing to a longer interaction time. When the tool shoulder enters in contact with the material, a steeper rise in tool temperature occurs since the larger contact area resulting in higher frictional heat. During the consolidation phase, the temperature further increases owing to a prolonged tool-material interaction, and the temperature reaches a peak value. However, at the beginning of the waiting phase, any further heat is produced since the rotation is stopped and negligible variation of temperature is appreciated since the high thermal inertia of the tool.

The trends of the plunging force and torque are reported in Fig. 3a. As can be inferred, the plunging force *Fz* shows a peak as the tool tip enters into contact with the (cold) upper sheet and then decreases due to the subsequent material softening; then, a second peak *F*max1 occurs at the beginning of the plunging phase when the plunging motion restarts since only a restricted layer of the material underlying the tool pin is heated. However, as the material becomes softer, the plunging force decreases and stabilizes around a steady state value FSS1. The force increases steeply as soon as the tool shoulder enters into contact with the underlying material and a second peak *F*max2 is shown. Thus, the tool further advances of 0.6 mm to enlarge the welded region but the plunging force decreases since the material softening. At the beginning of the consolidation phase, because any further axial displacement is produced, the plunging force drops and holds almost constant

Table 1 Welding parameters and ranges of variation

Symbol (n)	Welding parameter	Low level [−1]	High level [+1]
v_f (1)	Tool plunge rate [mm/min]	8	34
n (2)	Tool rotation speed [rpm]	900	2150
T_D (3)	Dwell time [s]	0	21
Tw	Waiting time [s]	7	
T_P	Pre-heating time [s]	7	

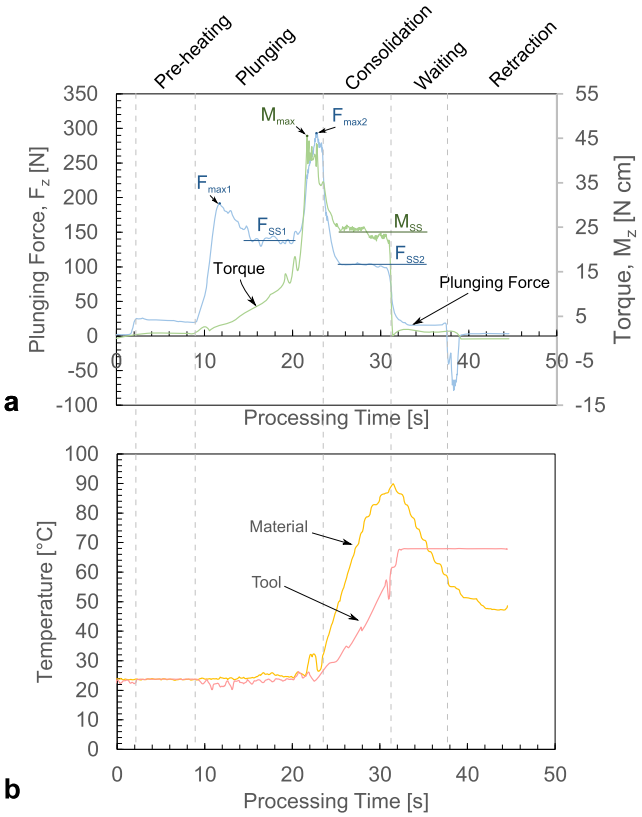

Fig. 3 Variation of **a** plunging force and torque and **b** material and tool temperatures during FSSW

(FSS2) during this phase. This force is required to stir and compress the material within the welding region. As the tool rotation stops, the plunging force drops almost to zero and it becomes negative as the tool is retracted owing to frictional forces exerted by the stirred material on the tool tip. It was observed that under any processing condition, except when the maximum plunging speed v_f=34 mm/min, FSS1 was lower than *F*max1. Actually, under the highest plunging speed (v_f=34 mm/min), the softening effect during the plunging phase was negligible leading to a slight reduction from *F*max1 and FSS1. Comparing the two above-mentioned peaks, it was observed that the second peak Fmax2 was always higher than *F*max1 since the larger contact surface of the tool shoulder as compared to the tool pin.

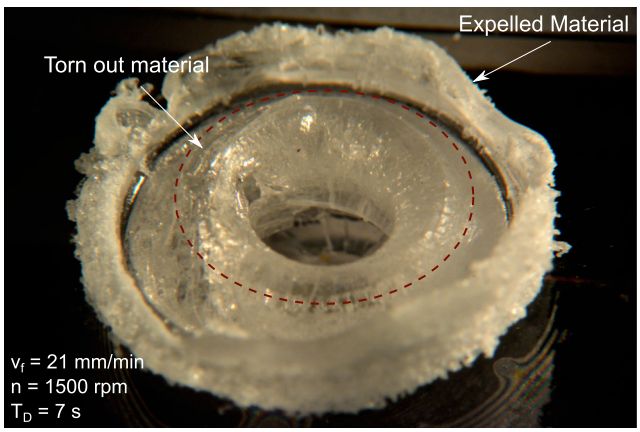

Fig. 4 Tear out effect owing to early tool retraction either excessively softened material

The variation of the torque during FSSW is reported in Fig. 3a. As can be observed, during pre-heating, the torque is almost zero owing to the small contact area of the tool tip and altogether with to the low contact pressure. On the other hand, during the plunging phase, the torque increases since the higher contact pressure (on the tool-tip flat face) and to the increase of the contact surface with the softened plastic material surrounding the tool-tip cylindrical surface. Consequently, as the tool shoulder enters into contact with the material, the torque shows a steeper increase since the contact surface becomes even larger. During the consolidation phase, the torque remains almost constant since the stirring action and drops to zero when the tool rotation is stopped (waiting time).

3.2 Effect of process parameters

In the following section, the effects of process parameters on plunging force, torque and temperatures (material and tool) are investigated.

3.2.1 Influence of the tool plunge rate

Figure 5 shows the effect of the plunging rate on the acquired signals (i.e. force, torque and temperatures) as well as the load-displacement curve during single lap shear tests. According to Fig. 5a–b, the increase in the plunging rate (v_f) leads to a reduction in the temperature of the material and that of the tool. Indeed, increasing the plunging rate from 8 to 34 mm/min results in a reduction of the maximum material temperature and that of the tool of 10 and 20 °C, respectively. Such a reduction is due to a shorter tool-workpiece interaction time (which reduces from 36 to 8.5 s) that leads to lower frictional heat dissipation.

The increase of the plunging speed influences the plunging force significantly. Indeed, the higher v_f, the higher the value of the first peak *F*max1 since the tool penetrates within a less softened material during the plunging phase. In addition, as the tool proceeds, the reduction in the plunging force owing to the material softening is attenuated for high values of v_f. As above-mentioned, at the maximum plunging speed, v_f= 34 mm/min, the steady state FSS1 is only slightly lower than the peak *F*max1. The increase in the plunging rate also results in an increase in the second peak *F*max2 since the lower material softening, while it has negligible influence on the steady state value FSS2 measured during the consolidation phase. Similarly, the variation of the plunging rate influences the torque only in the plunging phase (since the lower material softening) and the peak value *M*max, while it is negligible during consolidation phase (steady state value MSS).

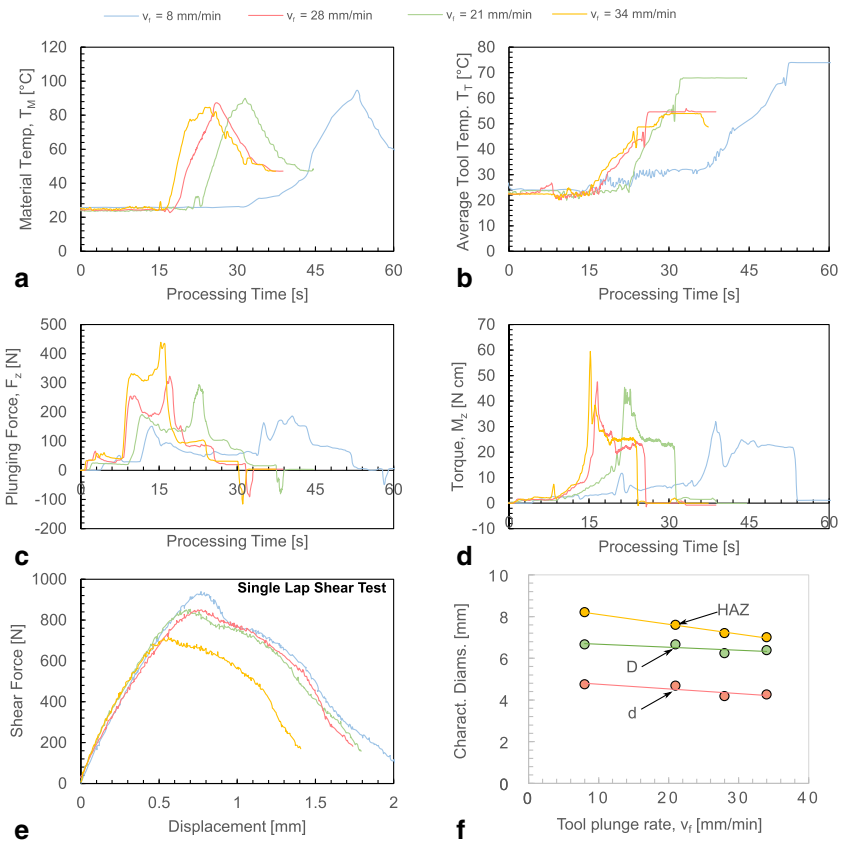

Fig. 5 Influence of plunging speed v_f on **a** material temperature, **b** tool temperature, **c** plunging force, **d** torque, **e** mechanical behaviour of the welds and **f** characteristic dimensions of the joints

The mechanical behaviour of welds performed by FSSW depends on the joints dimension and the material mixing quality. Figure 6 depicts the main regions that characterize the FSS welds. The welds are characterized by a keyhole (of diameter d), which is due to the penetration of the tool pin within the sheets, a welded region (of diameter D), which fastens the sheets, and a heat-affected zone (HAZ) surrounding the welded region, which is characterized by a material that was heated during the process but is not welded. As can be seen in Fig. 5e, the increase in the plunging rate has detrimental effects on the mechanical behaviour of the welds. Indeed, the lower frictional heat resulting from the reduced interactions time limits the dimension of the weld and consequently the shear strength and the toughness of the joint.

3.2.2 Influence of the tool rotational speed

The influence of the tool rotational speed (n) on the processing variables and mechanical behaviour of welds is depicted in Fig. 7. As can be inferred, the increase of n leads to a rise of the material and tool temperatures owing to higher frictional heat dissipation. The higher temperature produces higher material softening and, consequently, a reduction in all the characteristic values of the plunging force (Fmax1, FSS1, Fmax2 and FSS2) and torque (Mmax and MSS).

Because of the increase in material temperature and reduction in the plunging force with increasing the tool rotational speed, the mechanical behaviour of welded samples shows a peak at an intermediate level of n=1500 rpm. Indeed, at lower speeds, i.e. n=900 rpm and n=1260 rpm, poor material mixing is produced owing to low material softening; on the other hand, at higher speeds (i.e. n=2150 rpm), excessive material softening and ejection from the keyhole are produced, leading to a steep reduction in the plunging force FSS2 during the consolidation phase, which determines a reduction in the weld strength. Although increasing the tool rotational speed involves an enlargement of the welded region D, as depicted in Figs. 7f and 8, when increasing n from 1500 to 2150 rpm also results in an increase in the keyhole dimension owing to increasing inertia forces and lower material strength. Such a behaviour also contributes to reduce the joint strength when increasing the tool rotation speed over 1500 rpm.

3.2.3 Influence of the dwell time

During FSSW, the processing temperature shows a dramatic increase during the end of plunging phase and the consolidation owing to the larger tool-material contact surface (tools shoulder). As a result, when longer dwell times (T_D) (duration of consolidation phase) are adopted, higher material

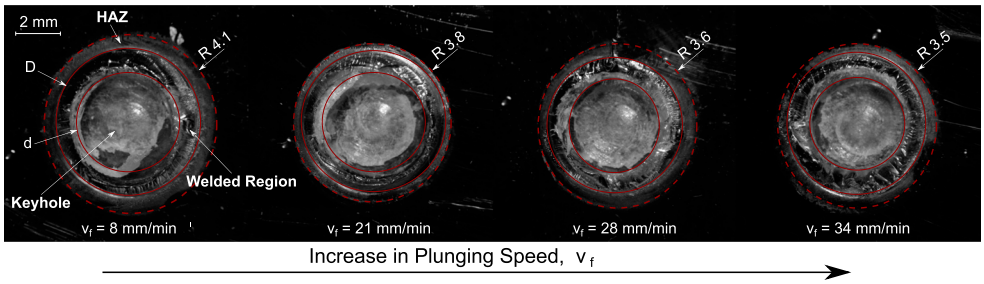

Fig. 6 Macrograph of typical regions of weld produced by FSSW as a function of the plunging speed, v_f

temperatures are produced as shown in Fig. 9a, b. Longer dwell times are used to increase the tool-material interaction and frictional heat production. Such a purpose can be also pursued by decreasing the plunging speed, even though the latter solution is less effective. Indeed, during the consolidation phase, the heat produced is higher than that produced during the plunging since the higher tool-material contact surface. Therefore, even a low increase in the dwell time produces a significant rise in the maximum material temperature. The influence of dwell time on maximum material temperature saturates for large values of T_D, as shown in Fig. 9a. However, under such conditions, prolonged consolidation phases result in a larger welded area (rather than increase in material temperature) as can be observed in Fig. 9f and on the macrographs depicted in Fig. 10. According to Fig. 9a, when the consolidation phase is avoided (T_D=0 s), a weld is produced even though a maximum material temperature (measured by the thermocouple) of almost 30 °C. Indeed, under such a condition, since the small interaction time, the heat produced at the tool-tip/material interface produces a steep gradient of temperature within a restricted region surrounding the tool tip. In this case, the temperature measured by the thermocouple is not representative of that arising within the welding.

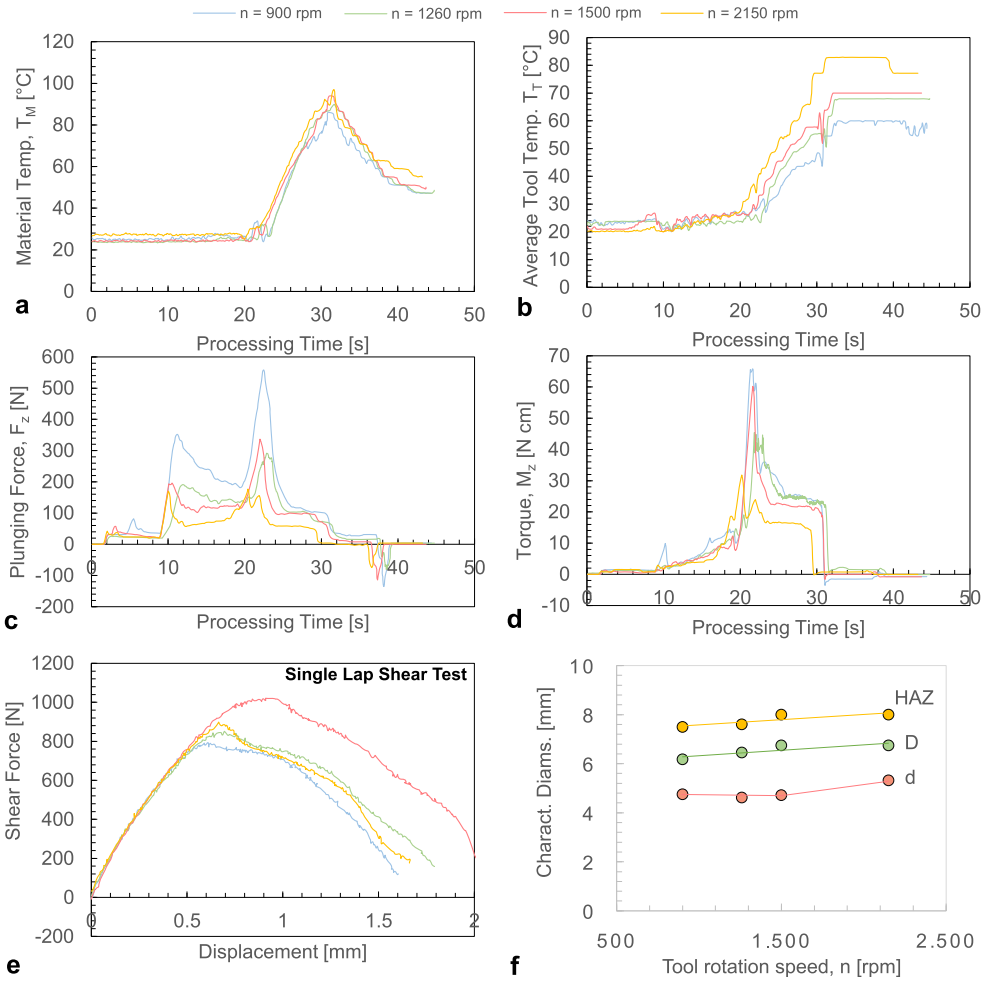

Fig. 7 Influence of tool rotation speed n on **a** material temperature, **b** tool temperature, **c** plunging force, **d** torque, **e** mechanical behaviour of the welds and **f** characteristic dimensions of the joints

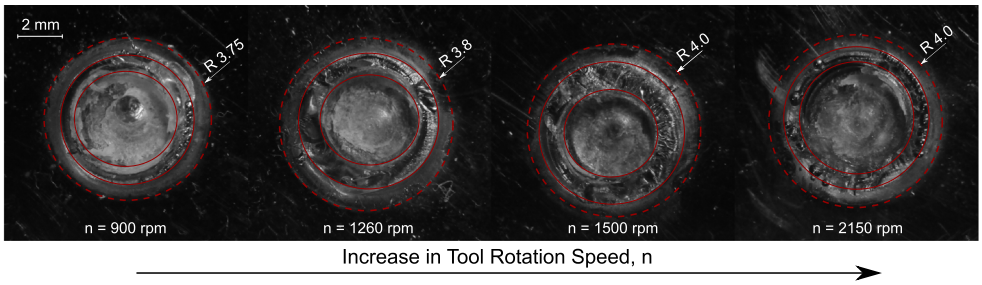

Fig. 8 Macrograph of typical regions of weld produced by FSSW varying the tool rotation speed, *n*

From Fig. 9c, d, it is noticeable that increasing the dwell time results in slight variation in the average plunging force and torque during the consolidation phase. In addition, increasing the dwell time leads to a rise in the material temperature and a significant enlargement of the welded region (Figs. 9f and 10) with beneficial effects on the mechanical behaviour of the produced welds as reported in Fig. 9e. Thus, increasing the dwell time represents a viable solution to increase the mechanical characteristics of the welds without weighting on the machine frame or requiring larger actuators.

3.3 Analysis of characteristic values

Figure 11 summarizes the influence of the process parameters on the characteristic values of the force, torque and temperatures. As can be seen, decreasing the tool plunge rate produces an almost linear reduction in the maximum plunging force *F*max2 and torque *M*max. A reduction of the plunging rate from the maximum v_f=34 mm/min to minimum value v_f= 8 mm/min determines a drop in the plunging force from 440 to 187 N, a decrement in the torque from 60 to 32 N cm. Lowering the tool plunge rate from the maximum to the

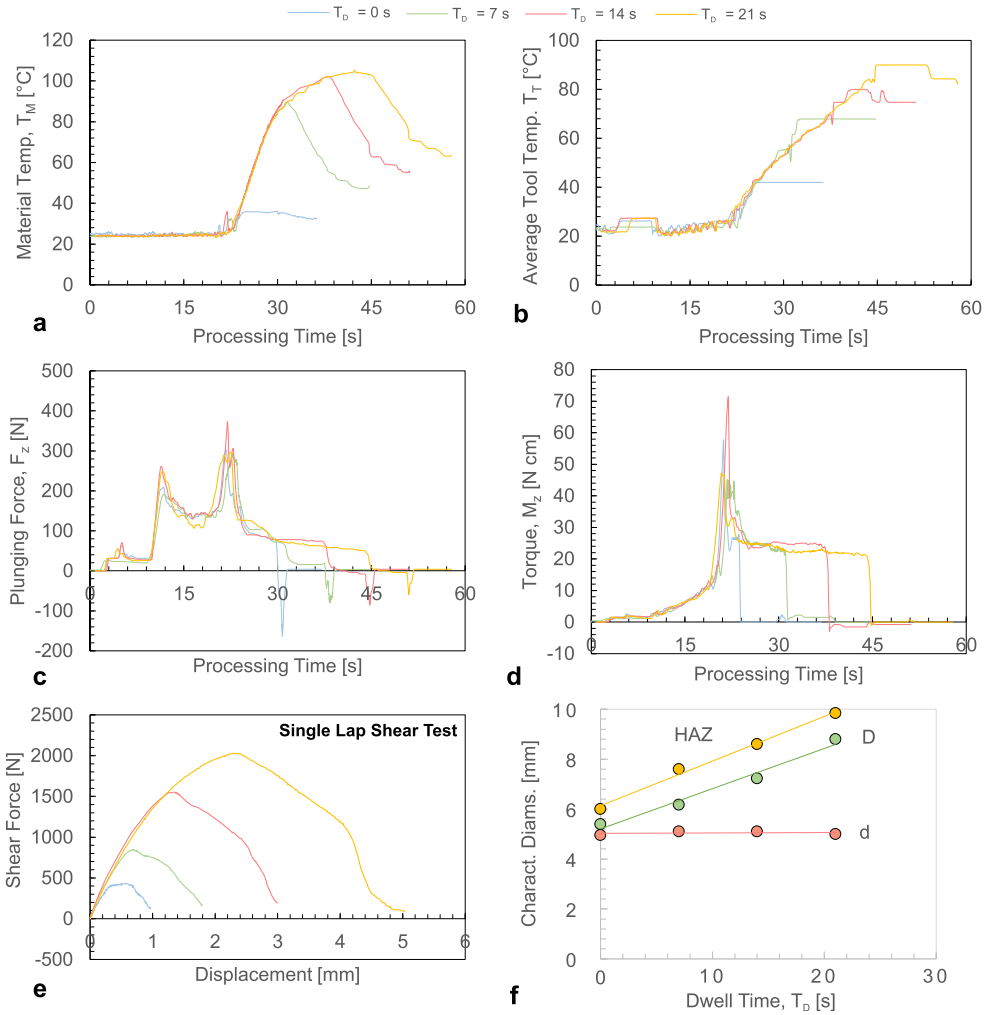

Fig. 9 Influence of dwell time T_D on **a** material temperature, **b** tool temperature, **c** plunging force, **d** torque, **e** mechanical behaviour of the welds and **f** characteristic dimensions of the joints

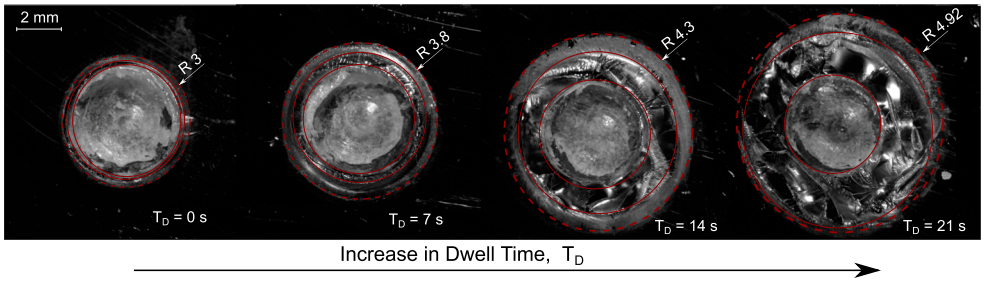

Fig. 10 Macrograph of typical regions of weld produced by FSSW varying the dwell time, T_D

minimum value produces an increase in temperatures (material/tool) from 85/54 to 95/74 °C while it influences the holding force FSS2 and torque MSS negligibly. Adopting low plunging speeds, other than reducing the force and the torque, is also beneficial for increasing the mechanical behaviour of the welds from 690 to 920 N.

According to Fig. 11, increasing n produces an exponential reduction in the plunging force and torque whose characteristic value Fzmax2 (Mmax) drops from 550 N (66 N cm) to 120 N (18 N cm). As shown in Fig. 7, the optimal value of n to which corresponds the highest value of the shear strength of the joint is n=

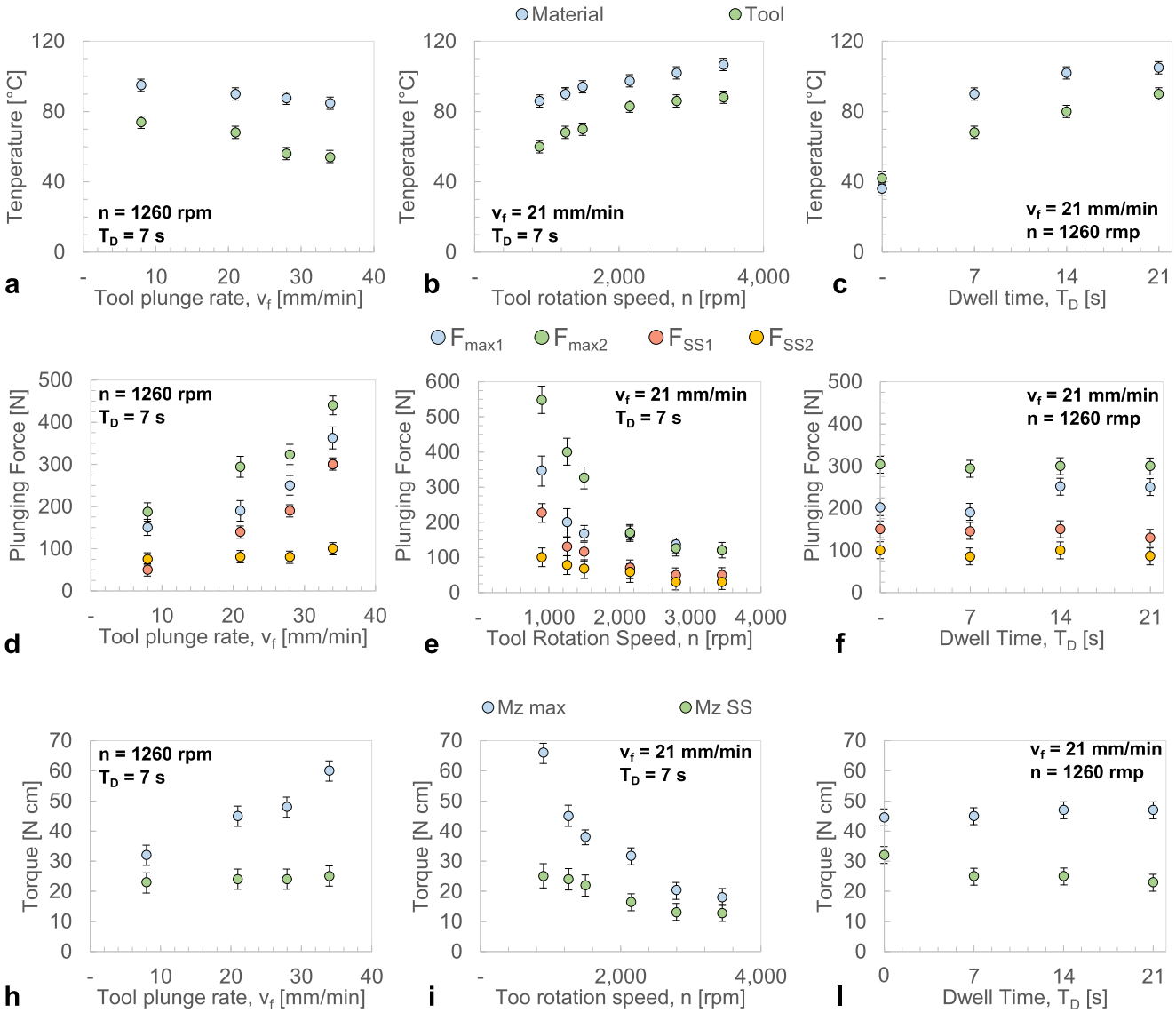

Fig. 11 Influence of process conditions on characteristic values of force, torque and temperatures

1500 rpm. Under such condition, the values of *F*zmax2 and *M*max are 327 N and 38 N cm, respectively.

The T_D has the highest influence on the material temperature, as can be inferred by comparing Fig. 11a–c. The material temperature, which highly influences the mechanical behaviour of the welds, shows a steep increase for low value of T_D, e.g. the maximum temperature Tmax produced with T_D=0 s is 36 °C while it rises up to 90 °C by increasing the dwell time by 7 s. The increase of Tmax with T_D saturates for values higher than 21 s and longer dwell time mainly results in enlarging the welding region. Since the dwell time represents the duration of the consolidation phase, it has no effect on the plunging phase. Nevertheless, according to Fig. 11f, i, varying the dwell time does not influence the FSS2 and MSS significantly.

3.4 Analysis of energy input

To better understand the effect of the analysed process parameters on the mechanical behaviour of the welded joints, an analysis concerning the input energy was carried out. Actually, during FSW and FSSW, the mechanical behaviour of welds depends on the quality of the stirring action as well as the dimension of the joint. Since in the performed experiments, the tool was not varied, the dimension of the welded region mainly depends on the process parameters and ultimately on the heat supplied. A series of analytical and numerical models were developed to evaluate the heat produced during FSW. Hamilton et al. [33] developed a thermal model for the evaluation of torque and input power for aluminium alloys. Prasanna et al. [34] and Luo et al. [35] calculated the contributes of the tool pin flat surface, tool shoulder and tool cylindrical surface to perform a numerical simulation of the temperature field during friction stir welding. However, the abovementioned models required the calibration of the coefficient of friction and its variation with temperature and pressure. During FSW process, the mechanical energy is converted into heat, which is used to weld the material, while only a small amount (lower than 10 %) is transferred to the tool [36]. Thus, the power introduced by the tool (*P*) can be obtained as the product of the torque by the angular rotation ϖ [37], and the input energy, *Q*, can be calculated by Eq. 1:

$$Q = \int M_Z \omega \, dt = \omega \int M_Z dt \tag{1}$$

where the integral is extended to the duration of the FSW process. Equation 1 was used to calculate the input energy under analysed process parameters. As can be observed, in Fig. 12, both the weld dimension and the weld strength are highly correlated with the input energy, the R^2 values being relatively close to the unity, proving that the input energy is strictly related to the mechanical behaviour of welded joints.

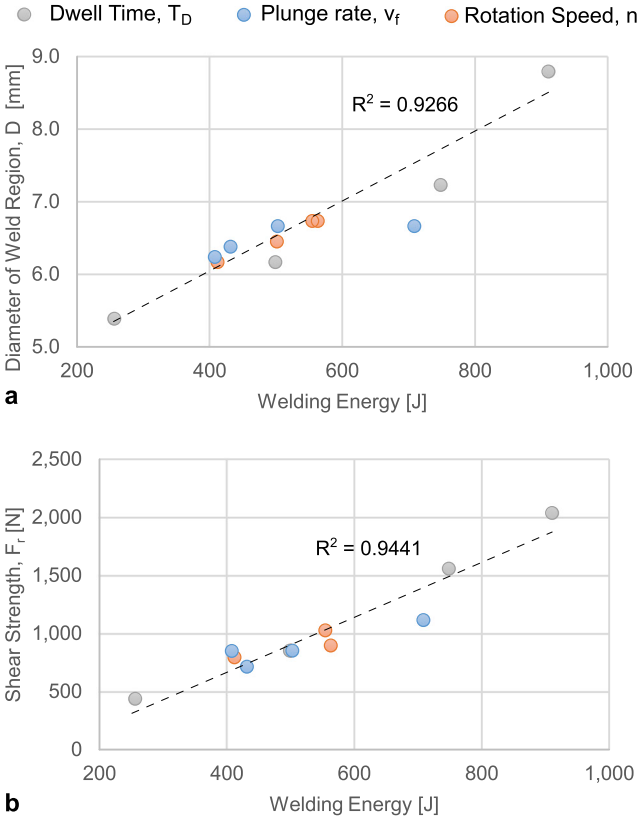

Fig. 12 Correlation of welding energy with **a** diameter of the weld and **b** shear strength

Therefore, the input energy was analysed (highlighting the contribute of the plunging phase) to better comprehend the influence of the process parameters on the joint quality. Figure 13 depicts the variation of the input energy with FSSW process parameters. According to Fig. 13a, increasing the tool rotation speed leads to higher supplied energy mainly during the plunging phase. On the other hand, the energy supplied during consolidation phase is influenced negligibly by variation of tool rotation speed since the increase of *n* comes with a higher material heating which results in torque reduction. As above-mentioned, excessive increase of *n* may result in excessive material ejection from the weld leading to a weakening of the weld. Therefore, increasing the tool rotational speed above 1500 rpm has both detrimental effects on the weld quality other than requiring more energy, thus reducing the efficiency of the process. On the other hand, the increase in the energy supplied by extending the consolidation either plunging phases (reducing the tool plunge rate) allows to improve the weld quality without any detrimental effect. Nevertheless, it appears by comparing Fig. 13b–c that increasing the dwell time would be preferable since higher power can be transferred to the material (stem from larger contact surface tool shoulder and higher distance from the tool axis) with evident advantages in terms of weld quality and productivity. As an example, increasing the dwell time by 21 s (from case 1 to

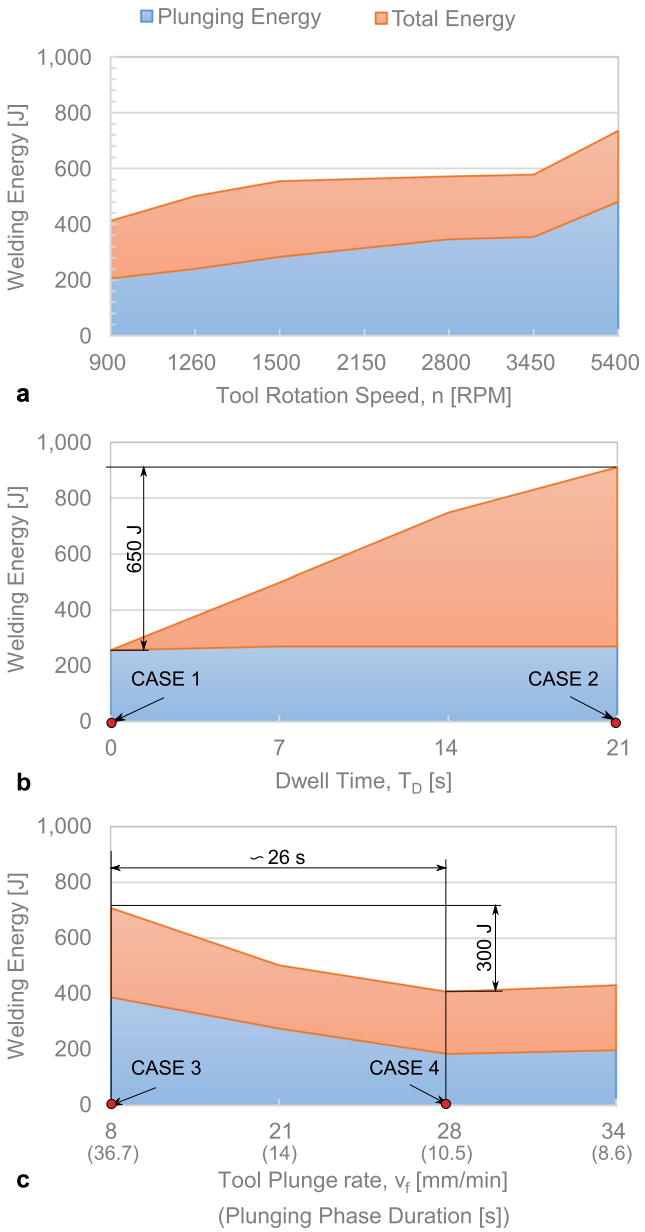

Fig. 13 Influence of process parameters on welding energy during FSSW highlighting the contribute of the plunging phase

case 2) would increase the transferred energy by 650 J while increasing the plunging duration by 26 s (from case 4 to case 3) involves an increase in the transferred energy by less than a half (300 J).

According to the achieved results, a procedure for the optimal selection of the process parameters aimed at maximizing the mechanical behaviour of the joints and reducing the processing time in FSSW can be drawn as follows:

1. Selection of the tool rotation speed, n: the optimal value of n allows increasing the material mixing action and temperature without causing material being ejected from the weld and waste of energy.
2. Selection of tool plunge rate, v_f: high values of tool plunge rate should be utilized in order to increase the process productivity. The contraction of the plunging phase can be exploited to extend the consolidation phase, which allows a faster heating transfer to the sheet material. Nevertheless, such a choice is constrained by the equipment limitations since the increase in the plunging rate comes with an increase in the plunging force.
3. Selection of the dwell time, T_D: the consolidation phase should be chosen in order to achieve the given mechanical strength of the joint.

In addition, since the high correlation between the input energy calculated by Eq. 1 and the mechanical behaviour of the welds, the product of the torque by the rotational speed could be utilized on an "Intelligent Sensored Machine" to perform an online correction of process parameters.

4 Conclusions

An instrumented drilling machine was developed to study the variation of the plunging force, torque and temperature in friction spot stir welding of polycarbonate sheets. The influence of tool rotational speed, plunging rate and dwell time was analysed. The main results are reported as follows:

- The increase in the plunging rate results in reduced tool-material interaction time and consequently lower process temperature. As a result, since the lower material softening, both the processing force and the torque are increased while the mechanical strength of the welds is decreased since the lower extension of the welding region.
- The increase in the tool rotation speed produces higher frictional heat and consequently higher material temperature and material softening. Consequently, the increase in tool rotational speed also comes with a reduction of the plunging force and torque since reduced material flow. As a result, the mechanical strength of the welds show a maximum at intermediate values of n resulting from a compromise of material temperature and applied plunging force during the consolidation phase. In addition, excessive tool rotation speed values cause material ejection which reduced the dimension of the weld area.
- Increasing the dwell time allows increasing the maximum temperature and extension of the welded area without influencing the plunging force and torque significantly. As a result, the strength of the welds increases almost linearly with the dwell time while the toughness increases more than linearly. Since the significant rise in material temperature when long consolidation phases are adopted, the waiting time should be also increased to in order to avoid extracting the tool from a pasty weld region, which

could result in weld damage. To this end, controlling the material temperature, rather than fixing the duration of the single processing phases using an instrumented machine could be beneficial to improve the weld quality.

- The analysis of the input energy allowed to understand more in depth the influence of the process parameters and their mutual relevance. In addition, the dimension and mechanical strength of the welds show a high correlation with the external energy. Thus, monitoring the torque and tool rotation speed during the FSSW could be beneficial to correct the process parameters either to predict the strength of the joint without performing destructive tests.

References

1. Lambiase F ((in Press)) Joinability of different thermoplastic polymers with aluminium AA6082 sheets by mechanical clinching. Int J Adv Manuf Technol
2. Lambiase F, Di Ilio A (2015) Mechanical clinching of metal–polymer joints. J Mater Process Technol 215:12–19
3. Settineri L, Atzeni E, Ippolito R (2010) Self piercing riveting for metal-polymer joints. Int J Mater Form 3(S1):995–998
4. Hussein FI, Akman E, Genc Oztoprak B, Gunes M, Gundogdu O, Kacar E, Hajim KI, Demir A (2013) Evaluation of PMMA joining to stainless steel 304 using pulsed Nd:YAG laser. Optics Laser Technol 49:143–152
5. Wirth FX, Zaeh MF, Krutzlinger M, Silvanus J (2014) Analysis of the bonding behavior and joining mechanism during friction press joining of aluminum alloys with thermoplastics. Procedia CIRP 18: 215–220
6. Blaga L, Bancilă R, dos Santos JF, Amancio-Filho ST (2013) Friction riveting of glass–fibre-reinforced polyetherimide composite and titanium grade 2 hybrid joints. Mater Des 50:825–829
7. Liu FC, Liao J, Nakata K (2014) Joining of metal to plastic using friction lap welding. Mater Des 54:236–244
8. He X, Gu F, Ball A (2014) A review of numerical analysis of friction stir welding. Prog Mater Sci 65:1–66
9. Shi L, Wu CS, Liu HJ (2014) Numerical analysis of heat generation and temperature field in reverse dual-rotation friction stir welding. Int J Adv Manuf Technol 74(1-4):319–334
10. Al-Roubaiy AO, Nabat SM, Batako ADL (2014) Experimental and theoretical analysis of friction stir welding of Al–Cu joints. Int J Adv Manuf Technol 71(9-12):1631–1642
11. Al-Badour F, Merah N, Shuaib A, Bazoune A (2014) Thermo-mechanical finite element model of friction stir welding of dissimilar alloys. Int J Adv Manuf Technol 72(5-8):607–617
12. Song X, Ke L, Xing L, Liu F, Huang C (2014) Effect of plunge speeds on hook geometries and mechanical properties in friction stir spot welding of A6061-T6 sheets. Int J Adv Manuf Technol 71(9-12):2003–2010
13. Papahn H, Bahemmat P, Haghpanahi M, Sommitsch C (2014) Study on governing parameters of thermal history during underwater friction stir welding. Int J Adv Manuf Technol 78(5-8):1101–1111
14. Ramulu PJ, Narayanan RG, Kailas SV (2013) Forming limit investigation of friction stir welded sheets: influence of shoulder diameter and plunge depth. Int J Adv Manuf Technol 69(9-12):2757–2772
15. Simões F, Rodrigues DM (2014) Material flow and thermo-mechanical conditions during Friction stir welding of polymers: literature review, experimental results and empirical analysis. Mater Des 59:344–351
16. Mostafapour A, Azarsa E (2012) A study on the role of processing parameters in joining polyethylene sheets via heat assisted friction stir welding: Investigating microstructure, tensile and flexural properties. Int J Phys Sci 7 (4)
17. Arora HS, Singh H, Dhindaw BK (2011) Composite fabrication using friction stir processing—a review. Int J Adv Manuf Technol 61(9-12):1043–1055
18. Oliveira PHF, Amancio-Filho ST, dos Santos JF, Hage E (2010) Preliminary study on the feasibility of friction spot welding in PMMA. Mater Lett 64(19):2098–2101
19. Bilici MK, Yükler Aİ, Kurtulmuş M (2011) The optimization of welding parameters for friction stir spot welding of high density polyethylene sheets. Mater Des 32(7):4074–4079
20. Bilici MK, Yükler Aİ (2012) Influence of tool geometry and process parameters on macrostructure and static strength in friction stir spot welded polyethylene sheets. Mater Des 33:145–152
21. Memduh K (2012) Friction stir spot welding parameters for polypropylene sheets. Sci Res Essays 7 (8)
22. Hoseinlaghab S, Mirjavadi SS, Sadeghian N, Jalili I, Azarbarmas M, Besharati Givi MK (2015) Influences of welding parameters on the quality and creep properties of friction stir welded polyethylene plates. Mater Des 67:369–378
23. Pirizadeh M, Azdast T, Rash Ahmadi S, Mamaghani Shishavan S, Bagheri A (2014) Friction stir welding of thermoplastics using a newly designed tool. Mater Des 54:342–347
24. Panneerselvam K, Lenin K (2014) Joining of Nylon 6 plate by friction stir welding process using threaded pin profile. Mater Des 53:302–307
25. Mendes N, Loureiro A, Martins C, Neto P, Pires JN (2014) Morphology and strength of acrylonitrile butadiene styrene welds performed by robotic friction stir welding. Mater Des 64:81–90
26. Mendes N, Neto P, Simão MA, Loureiro A, Pires JN (2014) A novel friction stir welding robotic platform: welding polymeric materials. Int J Adv Manuf Technol
27. Lambiase F, Di Ilio A, Paoletti A (2014) Optimization of friction stir welding of thermoplastics. In: Teti P (ed) 9th CIRP Conference on Intelligent Computation in Manufacturing Engineering - CIRP ICME '14, Ischia (Na). Italy
28. Junior WS, Emmler T, Abetz C, Handge UA, dos Santos JF, Amancio-Filho ST, Abetz V (2014) Friction spot welding of PMMA with PMMA/silica and PMMA/silica-g-PMMA nanocomposites functionalized via ATRP. Polymer 55(20):5146–5159
29. Junior WS, Handge UA, dos Santos JF, Abetz V, Amancio-Filho ST (2014) Feasibility study of friction spot welding of dissimilar single-lap joint between poly(methyl methacrylate) and poly(methyl methacrylate)-SiO2 nanocomposite. Mater Des 64: 246–250
30. Goushegir SM, dos Santos JF, Amancio-Filho ST (2014) Friction spot joining of aluminum AA2024/carbon-fiber reinforced poly(phenylene sulfide) composite single lap joints: microstructure and mechanical performance. Mater Des 54:196–206
31. Dashatan SH, Azdast T, Ahmadi SR, Bagheri A (2013) Friction stir spot welding of dissimilar polymethyl methacrylate and acrylonitrile butadiene styrene sheets. Mater Des 45:135–141
32. Lambiase F, Paoletti A, Di Ilio A (2015) Mechanical behaviour of friction stir spot welds of polycarbonate sheets. Int J Adv Manuf Technol:in Press
33. Hamilton C, Dymek S, Sommers A (2008) A thermal model of friction stir welding in aluminum alloys. Int J Mach Tools Manuf 48(10):1120–1130

34. Prasanna P, Rao BS, Rao GKM (2010) Finite element modeling for maximum temperature in friction stir welding and its validation. Int J Adv Manuf Technol 51(9-12):925–933
35. Luo J, Li S, Chen W, Xiang J, Wang H (2015) Simulation of aluminum alloy flowing in friction stir welding with a multiphysics field model. Int J Adv Manuf Technol
36. Nandan R, Roy GG, Debroy T (2006) Numerical simulation of three-dimensional heat transfer and plastic flow during friction stir welding. Metall Mater Trans A 37(4):1247–1259
37. Neto DM, Neto P (2012) Numerical modeling of friction stir welding process: a literature review. Int J Adv Manuf Technol